

# Temporal Parallelisation of Dynamic Programming and Linear Quadratic Control

Simo Särkkä, *Senior Member, IEEE*, Ángel F. García-Fernández

**Abstract**—This paper proposes a method for temporal parallelisation of dynamic programming solutions of optimal control problems. We also derive the temporal parallelisation of the linear quadratic tracking control problem. For these two problems, we derive the elements and associative operators to be able to use parallel scans to solve these problems with logarithmic time complexity rather than linear time complexity. The computational benefits of the parallel methods are demonstrated via numerical simulations run on a multi-core processor and a graphics processing unit.

**Index Terms**—Associative operator, dynamic programming, multi-core processing, optimal control, parallel computing, graphics processing unit

## I. INTRODUCTION

OPTIMAL control theory (see, e.g., [1]–[3]) is concerned with designing control signals to steer a system such that a given cost function is minimised, or equivalently, a performance measure is maximised. The system can be, for example, an airplane or autonomous vehicle which is steered to follow a given trajectory, an inventory system, a chemical reaction, or a mobile robot [1], [4]–[7].

Dynamic programming, in the form first introduced by Bellman 1950's, is a general method for determining feedback laws for optimal control and other sequential decision problems [3], [8]–[10], and it also forms the basis of reinforcement learning [7] which is a subfield of machine learning. The classic dynamic programming algorithm is a sequential procedure that proceeds backwards from the final time step to the initial time step, and determines the value (cost-to-go) function as well as the optimal control law in time complexity of  $O(T)$ , where  $T$  is the number of time steps. The algorithm is optimal in the sense that no sequential algorithm that processes all the  $T$  time steps can have a time-complexity less than  $O(T)$ .

However, the complexity  $O(T)$  is only optimal in a computer with one single-core central processing unit (CPU). Nowadays, even general-purpose computers typically have multi-core CPUs with tens of cores and higher-end computers can have hundreds of them. Furthermore, graphics processing

units (GPUs) have become common in accessories of general-purpose computers and current high-end GPUs can have tens of thousands of computational cores. Although single steps of the dynamic programming algorithm can be sped up by parallelisation enabled by the multiple cores [11], the dynamic programming algorithm still is inherently a sequential procedure which does not admit parallelisation in the time direction. This leads to time-complexity of  $O(T)$  also in multi-core architectures which is no longer optimal, because with aid of parallelisation we would expect to have a strictly sub-linear time-complexity.

The idea of parallelising dynamic programming for an allocation process can be found in [9, Sec. I.30]. Dynamic programming algorithms for discrete states that operate sequentially, but parallelise some of the computations are provided in [11], [12]. Various forms of parallel algorithms for dynamic programming with discrete states are given in [13]. Reference [14] presents a partitioned dynamic programming suitable for parallelisation for linear-quadratic problems, though it has the disadvantage that some required inverse matrices may not exist. An algorithm for decomposing an optimal control problem into subproblems with partially overlapping time windows is provided [15], and an approximate parallel algorithm for linear model predictive control (MPC) is given in [16]. Reference [17] provides combination rules to separate the dynamic programming algorithm into different subproblems across the temporal domain, which are the foundations for temporal parallelisation.

The contribution of this article is to present a parallel formulation of dynamic programming which reduces its time complexity down to  $O(\log T)$ . The central idea is to reformulate dynamic programming in terms of associative operators which allow for the use of parallel scan algorithms [18], [19] to parallelise the algorithm. The resulting algorithm has a span-complexity of  $O(\log T)$  which transforms into time-complexity of  $O(\log T)$  with large enough number of computational cores, and speeds up the computations significantly also in computers with a moderate number of cores. The general formulation is based on defining conditional value functions between two different time steps and combining them via the rule in [17]. We also specialise the methodology to discrete-state dynamic programming problems and to the linear-quadratic optimal control problem (i.e., linear quadratic tracker, LQT), which requires the propagation of the dual function [20] associated with the conditional value function. We also show how to obtain the optimal control laws and

S. Särkkä is with the Department of Electrical Engineering and Automation, Aalto University, 02150 Espoo, Finland (email: simo.sarkka@aalto.fi).

A. F. García-Fernández is with the Department of Electrical Engineering and Electronics, University of Liverpool, Liverpool L69 3GJ, United Kingdom, and also with the ARIES Research Centre, Universidad Antonio de Nebrija, Madrid, Spain (email: angel.garcia-fernandez@liverpool.ac.uk).

resulting trajectories making use of parallel computation. The parallel LQT algorithm is also extended to approximately solve certain nonlinear control problems by iterated linearisations, as in [21].

The present approach is closely related to the temporal parallelisation of Bayesian smoothers and hidden Markov model inference recently considered in [22]–[24]. These approaches use a similar scan-algorithm-based parallelisation in the context of state estimation problems. The combination rule is also related to so-called max-plus algebras for dynamic programming which have been considered, for example, in [25]–[28]. Finally, we empirically tested the algorithms by running them on multi-core CPU (24 cores) and GPU (~10k cores), and the results show that the algorithms provide significant speed up also in practice.

The structure of the paper is the following. In Section II we provide a brief background on dynamic programming and parallel computing, in Section III we provide the parallel methods to general and finite-state problems, in Section IV we consider the parallel solution to linear quadratic tracking control problem, in Section V we discuss some practical implementation aspects and computational complexity, in Section VI we experimentally illustrate the performance of the methods on CPU and GPU platforms, and finally in Section VII we conclude the article.

## II. BACKGROUND

In this section, we provide a brief background on optimal control and its dynamic programming solution, the linear quadratic control case, and associative operators in parallel computing.

### A. Deterministic control problem

The deterministic model that we consider consists of a difference equation and the corresponding cost function:

$$\begin{aligned} x_{k+1} &= f_k(x_k, u_k), \\ C[u_{S:T-1}] &= \ell_T(x_T) + \sum_{n=S}^{T-1} \ell_n(x_n, u_n), \end{aligned} \quad (1)$$

where, for  $k = S, \dots, T$ ,  $x_k$  is the state (typically  $x_k \in \mathbb{R}^{n_x}$ ),  $f_k(\cdot)$  is the function that models the state dynamics at time step  $k$ ,  $u_{S:T-1} = (u_S, \dots, u_{T-1})$  is the control/decision sequence (typically  $u_k \in \mathbb{R}^{n_u}$  with  $n_u \leq n_x$ ), and  $\ell_k(\cdot)$  is a lower bounded function that indicates the cost at time step  $k$ . The initial state  $x_S$  is known. The aim is now to find a feedback control law or policy  $u_k(x_k)$  such that if at step  $k$  the state is  $x_k$ , the cost function  $C[u_{S:T-1}]$  for the steps from  $S$  to  $T$  is minimized with the sequence  $u_S(x_S), \dots, u_T(x_T)$ .

In Bellman's dynamic programming [3], [8], [9] the idea is to form a cost-to-go or value function  $V_k(x_k)$  which gives the cost of the trajectory when we follow the optimal decisions for the remaining steps up to  $T$  starting from state  $x_k$ . It can be shown [8] that the value function admits the recursion

$$V_k(x_k) = \min_{u_k} \{ \ell_k(x_k, u_k) + V_{k+1}(f_k(x_k, u_k)) \} \quad (2)$$

with  $V_T(x_T) = \ell_T(x_T)$ , which determines the optimal control law via

$$u_k(x_k) = \arg \min_{u_k} \{ \ell_k(x_k, u_k) + V_{k+1}(f_k(x_k, u_k)) \}. \quad (3)$$

Given the control law (3) for all time steps, we can compute the optimal trajectory from time steps  $S + 1$  to  $T$ , which is denoted as  $(x_{S+1}^*, \dots, x_T^*)$ , by an additional forward pass starting at  $x_S^* = x_S$  and

$$x_{k+1}^* = f_k(x_k^*, u_k(x_k^*)) = f_k^*(x_k^*). \quad (4)$$

### B. Linear quadratic tracker

The linear quadratic tracker (LQT) [2] is the solution to a linear-quadratic control problem of the form

$$\begin{aligned} x_{k+1} &= F_k x_k + c_k + L_k u_k, \\ \ell_T(x_T) &= \frac{1}{2} (H_T x_T - r_T)^\top X_T (H_T x_T - r_T) \\ \ell_n(x_n, u_n) &= \frac{1}{2} (H_n x_n - r_n)^\top X_n (H_n x_n - r_n) + \frac{1}{2} u_n^\top U_n u_n, \end{aligned} \quad (5)$$

where we assume that  $X_n \geq 0$ ,  $U_n > 0$ , and that they are symmetric matrices.

In this setting, the objective is that a linear combination of the states  $H_k x_k$  follows a reference trajectory  $r_k$  from time step  $S$  to  $T$ . The linear quadratic regulator is a special case of the LQT problem by setting  $r_k = 0$ ,  $c_k = 0$ , and  $H_k = I \forall k$ .

In this case, the value function is

$$V_k(x_k) = z + \frac{1}{2} x_k^\top S_k x_k - v_k^\top x_k, \quad (6)$$

where  $v_k$  is an  $n_x \times 1$  vector and  $S_k$  is an  $n_x \times n_x$  symmetric matrix and, throughout the paper, we use  $z$  to denote an undetermined constant that does not affect the calculations. The parameters  $v_k$  and  $S_k$  can be obtained recursively backwards. Starting with  $v_T = H_T^\top X_T r_T$  and  $S_T = H_T^\top X_T H_T$ , we obtain

$$v_k = (F_k - L_k K_k)^\top (v_{k+1} - S_{k+1} c_k) + H_k^\top X_k r_k, \quad (7)$$

$$S_k = F_k^\top S_{k+1} (F_k - L_k K_k) + H_k^\top X_k H_k, \quad (8)$$

where

$$K_k = (L_k^\top S_{k+1} L_k + U_k)^{-1} L_k^\top S_{k+1} F_k. \quad (9)$$

The optimal control law is

$$u_k = -K_k x_k + K_k^v v_{k+1} - K_k^c c_k, \quad (10)$$

where

$$K_k^v = (L_k^\top S_{k+1} L_k + U_k)^{-1} L_k^\top, \quad (11)$$

$$K_k^c = (L_k^\top S_{k+1} L_k + U_k)^{-1} L_k^\top S_{k+1} c_k. \quad (12)$$

The optimal trajectory resulting from applying the optimal control law (10) can be computed with an additional forward pass (4) starting at  $x_S$  and with control law (10).

It should be noted that the derivation of LQT in [2] does not include time-varying matrices or parameter  $c_k$  in the problem formulation (5), but it is straightforward to include these. It is also possible to use the LQT solution as a basis for approximate non-linear control by linearizing the system along a nominal trajectory (see [1], [21], [29] and Sec. IV-D.3).

### C. Associative operators and parallel computing

Parallel computing (see, e.g., [30], [31]) refers to programming and algorithm design methods that take the availability of multiple computational cores or computers into account. When some parts of the problem can be solved independently, then those parts can be solved in parallel which reduces the total computational time. The more parts we can solve in parallel, the more speed up we get.

Sequential problems which at the first glance do not seem to be parallelisable can often be parallelised using so called parallel scan or all-prefix-sums algorithms [18], [19]. The problem that these algorithm solve is that given a sequence of elements  $a_1, \dots, a_T$  and an associative operator such as summation  $+$  defined on them, the parallel scan algorithm solves the following all prefix sums

$$\begin{aligned} s_1 &= a_1, \\ s_2 &= a_1 + a_2, \\ s_3 &= a_1 + a_2 + a_3, \\ &\dots \\ s_T &= a_1 + a_3 + \dots + a_T, \end{aligned} \quad (13)$$

very fast – in  $O(\log T)$  time – by using parallel computing. The key trick is that because the operator is associative, we can rearrange the computations in various ways which generate independent sub-problems, for example,

$$((a_1 + a_2) + a_3) + a_4 = (a_1 + a_2) + (a_3 + a_4), \quad (14)$$

and by a suitable combination of the partial solutions we can obtain the result in  $O(\log T)$  parallel steps.

The parallel scan algorithm does not require the associative operator to be summation, but it can also be applied to other associative operators such as matrix multiplications or minimisations. Furthermore, the prefix sums can also be computed in backward direction  $(a_1 + \dots + a_T, \dots, a_{T-1} + a_T, a_T)$ . In articles [22]–[24] it was shown how it is possible to define associative operators and elements for state-estimation problems such that the computations of forward and backward prefix sums (in parallel) correspond to computing the filtering and smoothing solutions to state estimation problems. The aim of this article is to define the associative operators and elements which allow for similar reduction of dynamic programming to prefix sum computations.

## III. PARALLEL OPTIMAL CONTROL

In this section, we start by defining conditional value functions and their combination rules and then we use them to define the associative operators and elements for parallelisation. We also discuss the parallel solution of the optimal trajectory, and finally, we discuss the special case of when the state space and controls take values in finite sets.

### A. Conditional value functions and combination rules

Our aim is now to present alternative formulations of the value function recursions in terms of conditional value functions that are useful to designing the parallel algorithms.

Central to our exposition is the conditional value function which we define as follows.

**Definition 1 (Conditional value function):** The conditional value function  $V_{k \rightarrow i}(x_k, x_i)$  is the cost of the optimal trajectory starting from  $x_k$  and ending at  $x_i$ , that is

$$V_{k \rightarrow i}(x_k, x_i) = \min_{u_{k:i-1}} \sum_{n=k}^{i-1} \ell_n(x_n, u_n) \quad (15)$$

subject to

$$x_n = f_{n-1}(x_{n-1}, u_{n-1}) \quad \forall n \in \{k+1, \dots, i\}. \quad (16)$$

If there is no path connecting  $x_k$  and  $x_i$ , then the constraint (16) cannot be met and  $V_{k \rightarrow i}(x_k, x_i) = \infty$ .

The combination rule for conditional value functions is provided in the following theorem.

**Theorem 2:** The recursions for the value functions and conditional value functions can be written as

$$V_{k \rightarrow i}(x_k, x_i) = \min_{x_j} \{V_{k \rightarrow j}(x_k, x_j) + V_{j \rightarrow i}(x_j, x_i)\}, \quad (17)$$

for  $k < j < i \leq T$  and

$$V_k(x_k) = \min_{x_i} \{V_{k \rightarrow i}(x_k, x_i) + V_i(x_i)\}, \quad (18)$$

for  $k < i \leq T$ .

*Proof:* See Appendix I. ■

As part of the minimisation in (18), we also get the minimizing state  $x_i$ . Due to the principle of optimality, this value is the state at time step  $i$  that is on the optimal trajectory from  $x_k$  until time  $T$ . Similarly, the argument of minimisation  $x_j$  in (17) is part of the optimal trajectory from  $x_k$  to  $x_i$ .

### B. Associative operator for value functions

The associative element  $a$  of the parallel scan algorithm is defined to be a conditional value function  $V_a(\cdot, \cdot) : \mathbb{R}^{n_x} \times \mathbb{R}^{n_x} \rightarrow \mathbb{R}$  such that

$$a = V_a(x, y). \quad (19)$$

The combination rule for two elements  $a = V_a(x, y)$  and  $b = V_b(x, y)$  is then given as follows.

**Definition 3:** Given elements  $a$  and  $b$  of the form (19), the binary associative operator for dynamic programming is

$$a \otimes b \triangleq \min_z \{V_a(x, z) + V_b(z, y)\}. \quad (20)$$

This operator is an associative operator because min operation is associative. This is summarized in the following lemma.

**Lemma 4:** The operator in Definition 3 is associative.

*Proof:* For three elements  $a$ ,  $b$ , and  $c$ , we have

$$\begin{aligned} (a \otimes b) \otimes c &\triangleq \min_{z'} \left\{ \min_z \{V_a(x, z) + V_b(z, z')\} + V_c(z', y) \right\} \\ &= \min_z \left\{ V_a(x, z) + \min_{z'} \{V_b(z, z') + V_c(z', y)\} \right\} \\ &\triangleq a \otimes (b \otimes c), \end{aligned} \quad (21)$$

which thus shows that  $(a \otimes b) \otimes c = a \otimes (b \otimes c)$ . ■

The elements and combination rule allows us to construct the conditional and conventional value functions as follows.

*Theorem 5:* If we initialize elements  $a_k$  for  $k = S, \dots, T$  as follows:

$$a_k = V_{k \rightarrow k+1}(x_k, x_{k+1}), \quad (22)$$

where  $V_{T \rightarrow T+1}(x_T, x_{T+1}) \triangleq V_T(x_T)$ , then

$$a_S \otimes a_{S+1} \otimes \dots \otimes a_{k-1} = V_{S \rightarrow k}(x_S, x_k) \quad (23)$$

and

$$a_k \otimes a_{i+1} \otimes \dots \otimes a_T = V_k(x_k). \quad (24)$$

*Proof:* The first identity results from sequential application of (17) forward, and the second from sequential application (18) backwards. ■

This result implies that we can compute the value function  $V_k(\cdot)$  by initializing elements as in Theorem 5 and by applying a sequence of associative operations in Definition 3 on the elements. Because the initialisation is fully parallelisable, and the associative operations are parallelisable (via the scan algorithm), this provides us the means to compute all the values functions in parallel.

*Remark 6:* After computing all the value functions, we can form the control laws  $u_k(x_k)$  independently for each  $k$  by using (3).

*Remark 7:* If we are interested in evaluating  $V_{S \rightarrow k}(x_S, x_k)$  at a given  $x_S$ , as we are in the trajectory recovery, then instead of first using (23) with initialisation (22), and then evaluating the result at  $x_S$ , we can also initialise with

$$a_{S-1} = V_{S-1 \rightarrow S}(x, x') = \begin{cases} 0 & \text{if } x' = x_S, \\ \infty & \text{otherwise.} \end{cases} \quad (25)$$

### C. Optimal trajectory recovery

Once we have obtained the optimal control laws (3) in parallel, we can compute the resulting optimal trajectory  $(x_{S+1}^*, \dots, x_T^*)$  in parallel using two methods.

**1) Method 1:** In the first method for trajectory recovery, the state of the optimal trajectory at time step  $k$  can be computed by using (4) and the composition of functions

$$x_k^* = (f_{k-1}^* \circ \dots \circ f_{S+1}^* \circ f_S^*)(x_S). \quad (26)$$

We can compute (26) using parallel scans as follows. The associative element  $a$  is defined to be a function on  $x$ ,  $a = f_a(\cdot)$  and the operator is the function composition, which is associative [32], in the following definition.

*Definition 8:* Given elements  $a = f_a(\cdot)$  and  $b = f_b(\cdot)$ , the binary associative operator for optimal trajectory recovery is

$$a \otimes b \triangleq f_b \circ f_a \quad (27)$$

where  $\circ$  denotes the composition of two functions. We should note that the order of the function composition is reverted. Then, we can recover the optimal trajectory via the following lemma.

*Lemma 9:* If we initialize element  $a_S$  as the function  $f_S^*(\cdot)$ , which is given by (4), evaluated at  $x_S$

$$a_S = f_S^*(x_S), \quad (28)$$

and, for  $k = S+1, \dots, T-1$ ,  $a_k$  is initialised as the function

$$a_k = f_k^*(\cdot), \quad (29)$$

then

$$a_S \otimes a_{S+1} \otimes \dots \otimes a_{k-1} = x_k^*, \quad (30)$$

where  $x_k^*$  is the state of the optimal trajectory at time step  $k$ .

**2) Method 2:** An alternative method, which resembles the max-product algorithm in probabilistic graphical models [33], is to notice that from the definition of the conditional value function (15) and the value function (2), the state of the optimal trajectory at time step  $k$  is given by

$$x_k^* = \arg \min_{x_k} \{V_{S \rightarrow k}(x_S, x_k) + V_k(x_k)\}, \quad (31)$$

where we recall that  $x_S$  is the initial known state. That is, we can just minimise the sum of the forward conditional value function  $V_{S \rightarrow k}(x_S, x_k)$  and the (backwards) value function  $V_k(x_k)$ , which can be calculated using parallel scans via (23) and (24), respectively. Then, the minimisation (31) can be done for each node in parallel.

It should be noted that both approaches for optimal trajectory recovery require two parallel scans, one forward and one backwards.

### D. Finite state and control spaces

The case in which the state and the control input belong to finite state spaces is important as we can solve the control problem in both sequential and parallel forms in closed-form. Let  $x_k \in \{1, \dots, D_x\}$  and  $u_k \in \{1, \dots, D_u\}$  where  $D_x$  and  $D_u$  are natural numbers. Then,  $f_k(x_k, u_k)$  and  $\ell_n(x_n, u_n)$  can be represented by matrices of dimensions  $D_x \times D_u$ ,  $V_k(x_k)$  by a vector of dimension  $D_x$ ,  $u_k(x_k)$  by a vector of dimension  $D_x$ , and  $V_{k \rightarrow i}(x_k, x_i)$  by a matrix of size  $D_x \times D_x$ . Due to the finite state space, the required minimisations in (2) and (20), can be performed by exhaustive search, which can also be parallelised.

For Method 1 for optimal trajectory recovery, the function  $f_k^*(\cdot)$  can be represented as a vector of dimension  $D_x$ , and the function composition in (31) can be performed by evaluating all cases.

## IV. PARALLEL LINEAR QUADRATIC TRACKER (LQT)

In this section, we provide the parallel solution to the linear quadratic optimal control problem, the parallel linear quadratic tracker (LQT). We first derive the associative operators and elements for value function and trajectory computation for the general LQT. We then discuss extensions to stochastic and non-linear problems.

### A. Conditional value functions and combination rules

For the LQT problem in (5),  $V_{k \rightarrow i}(x_k, x_i)$  in (15) is a quadratic program with affine equality constraints [20] that we represent by its dual problem

$$V_{k \rightarrow i}(x_k, x_i) = \max_{\lambda} g_{k \rightarrow i}(\lambda; x_k, x_i), \quad (32)$$



where the dual function  $g_{k \rightarrow i}(\cdot, \cdot, \cdot)$  has the parameterisation

$$g_{k \rightarrow i}(\lambda; x_k, x_i) = z + \frac{1}{2} x_k^\top J_{k,i} x_k - x_k^\top \eta_{k,i} - \frac{1}{2} \lambda^\top C_{k,i} \lambda - \lambda^\top (x_i - A_{k,i} x_k - b_{k,i}). \quad (33)$$

If  $C_{k,i}$  is invertible, one can solve (32) by calculating the gradient of (33) w.r.t.  $\lambda$  and setting it equal to zero, to obtain

$$\begin{aligned} V_{k \rightarrow i}(x_k, x_i) &= z + \frac{1}{2} x_k^\top J_{k,i} x_k - x_k^\top \eta_{k,i} \\ &+ \frac{1}{2} (x_i - A_{k,i} x_k - b_{k,i})^\top C_{k,i}^{-1} (x_i - A_{k,i} x_k - b_{k,i}). \end{aligned} \quad (34)$$

In this case, we can also interpret the conditional value function (34) in terms of conditional Gaussian distributions as

$$\begin{aligned} &\exp(-V_{k \rightarrow i}(x_k, x_i)) \\ &\propto N(x_i; A_{k,i} x_k + b_{k,i}, C_{k,i}) N_I(x_k; \eta_{k,i}, J_{k,i}) \end{aligned} \quad (35)$$

where  $N(\cdot; \bar{x}, P)$  denotes a Gaussian density with mean  $\bar{x}$  and covariance matrix  $P$ , and  $N_I(\cdot; \eta, J)$  denotes a Gaussian density parameterised in information form with information vector  $\eta$  and information matrix  $J$ . A Gaussian distribution with mean  $\bar{x}$  and covariance matrix  $P$ , can be written in its information form as  $\eta = P^{-1}\bar{x}$  and  $J = P^{-1}$ .

Nevertheless, in general  $C_{k,i}$  is not invertible so it is suitable to keep the dual function parameterisation in (32).

**Lemma 10:** Given two elements  $V_{k \rightarrow j}(x_k, x_j)$  and  $V_{j \rightarrow i}(x_j, x_i)$  of the form (32), their combination  $V_{k \rightarrow i}(x_k, x_i)$ , which is obtained using Theorem 2, is of the form (32) and characterised by

$$\begin{aligned} A_{k,i} &= A_{j,i} (I + C_{k,j} J_{j,i})^{-1} A_{k,j}, \\ b_{k,i} &= A_{j,i} (I + C_{k,j} J_{j,i})^{-1} (b_{k,j} + C_{k,j} \eta_{j,i}) + b_{j,i}, \\ C_{k,i} &= A_{j,i} (I + C_{k,j} J_{j,i})^{-1} C_{k,j} A_{j,i}^\top + C_{j,i}, \\ \eta_{k,i} &= A_{k,j}^\top (I + J_{j,i} C_{k,j})^{-1} (\eta_{j,i} - J_{j,i} b_{k,j}) + \eta_{k,j}, \\ J_{k,i} &= A_{k,j}^\top (I + J_{j,i} C_{k,j})^{-1} J_{j,i} A_{k,j} + J_{k,j}. \end{aligned} \quad (36)$$

where  $I$  is an identity matrix of size  $n_x$ .

The proof is provided in Appendix I-B. It should be noted that the combination rule (36) is equivalent to the combination rule for the parallel linear and Gaussian filter, which also considers Gaussian densities of the form (35) [22, Lem. 8].

## B. Associative operator for value functions

The following lemma establishes how to define the elements of the parallel scan algorithms to obtain the value functions  $V_{S \rightarrow k}(x_S, x_k)$  and  $V_k(x_k)$ .

**Lemma 11:** If we initialize elements  $a_k$  for  $k = S, \dots, T$  as follows:

$$a_k = V_{k \rightarrow k+1}(x_k, x_{k+1}), \quad (37)$$

where  $V_{k \rightarrow k+1}(x_k, x_{k+1})$  is of the form (32) with

$$\begin{aligned} A_{k,k+1} &= F_k, \\ b_{k,k+1} &= c_k, \\ C_{k,k+1} &= L_k U_k^{-1} L_k^\top, \\ \eta_{k,k+1} &= H_k^\top X_k r_k, \\ J_{k,k+1} &= H_k^\top X_k H_k, \end{aligned} \quad (38)$$

for  $k = S, \dots, T-1$  and  $V_{T \rightarrow T+1}(x_T, x_{T+1})$  has parameters

$$\begin{aligned} A_{T,T+1} &= 0, \\ b_{T,T+1} &= 0, \\ C_{T,T+1} &= 0, \\ \eta_{T,T+1} &= H_T^\top r_T, \\ J_{T,T+1} &= H_T^\top X_T H_T, \end{aligned} \quad (39)$$

then,

$$a_S \otimes a_{S+1} \otimes \dots \otimes a_{k-1} = V_{S \rightarrow k}(x_S, x_k), \quad (40)$$

and

$$a_k \otimes a_{i+1} \otimes \dots \otimes a_T = V_{k \rightarrow T+1}(x_k, x_{T+1}). \quad (41)$$

where

$$V_{k \rightarrow T+1}(x_k, 0) = V_k(x_k). \quad (42)$$

Furthermore,  $V_k(x_k)$  is of the form (6) with

$$\begin{aligned} S_k &= J_{k,T+1}, \\ v_k &= \eta_{k,T+1}. \end{aligned} \quad (43)$$

*Proof:* This lemma is proved in Appendix I-C. ■

Once we obtain  $v_{k+1}$  and  $S_{k+1}$  using Lemma 11, we can compute the optimal control  $u_k$  using (10).

**Remark 12:** If we are interested in evaluating the conditional value functions  $V_{S \rightarrow k}(x_S, x_k)$  for a given  $x_S$ , then we can also directly initialise by

$$\begin{aligned} A_{S-1,S} &= 0, \\ b_{S-1,S} &= x_S, \\ C_{S-1,S} &= 0, \\ \eta_{S-1,S} &= 0, \\ J_{S-1,S} &= 0. \end{aligned} \quad (44)$$

## C. Optimal trajectory recovery

We proceed to explain how the two optimal trajectory recovery methods explained in Section III-C work for the LQT problem.

**1) Method 1:** Plugging the optimal control law (10) into the dynamic equation in (5), the optimal trajectory function in (4) becomes

$$f_k^*(x_k) = \tilde{F}_k x_k + \tilde{c}_k, \quad (45)$$

where

$$\tilde{F}_k = F_k - L_k K_k \quad (46)$$

$$\tilde{c}_k = c_k + L_k K_k^v v_{k+1} - L_k K_k^c c_k. \quad (47)$$

We denote a conditional optimal trajectory from time step  $k$  to  $i$  as

$$f_{k \rightarrow j}^*(x_k, x_j) = (f_{j-1}^* \circ \dots \circ f_{k+1}^* \circ f_k^*)(x_k) \quad (48)$$

$$= \tilde{F}_{k,j}x_k + \tilde{c}_{k,j}. \quad (49)$$

**Lemma 13:** Given two elements  $f_{k \rightarrow j}^*(x_k, x_j)$  and  $f_{j \rightarrow i}^*(x_j, x_i)$  of the form (49), their combination  $f_{k \rightarrow i}^*(x_k, x_i)$ , given by Definition 8, is a function  $f_{k \rightarrow i}^*(x_k, x_i)$  of the form (49) with

$$\tilde{F}_{k,i} = \tilde{F}_{j,i}\tilde{F}_{k,j}, \quad (50)$$

$$\tilde{c}_{k,i} = \tilde{F}_{j,i}\tilde{c}_{k,j} + \tilde{c}_{j,i}. \quad (51)$$

*Proof:* The proof of this lemma is direct by using function compositions. ■

How to recover the optimal trajectory using parallel scans is indicated in the following lemma.

**Lemma 14:** If we initialise the elements of the parallel scan as  $a_k = f_{k \rightarrow k+1}^*(x_k)$ , with

$$\tilde{F}_{k,k+1} = \tilde{F}_k, \quad (52)$$

$$\tilde{c}_{k,k+1} = \tilde{c}_k, \quad (53)$$

for  $k \in \{S+1, \dots, T-1\}$ , and, for  $k = S$ , we set  $\tilde{F}_{S,S+1} = 0$  and  $\tilde{c}_{S,S+1} = \tilde{F}_Sx_S + \tilde{c}_S$ , then,

$$a_{k-1} \otimes a_{k-2} \otimes \dots \otimes a_S = x_k^* \quad (54)$$

where  $x_k^*$  is the state of the optimal trajectory at time step  $k$ .

**2) Method 2:** This method makes use of (31) to recover the optimal trajectory. It first runs a forward pass to compute  $V_{S \rightarrow k}(x_S, x_k)$  and then a backward pass to compute  $V_k(x_k)$ . Then, the optimal trajectory is obtained via the following lemma.

**Lemma 15:** Given  $V_k(x_k)$  of the form (6) and  $V_{S \rightarrow k}(x_S, x_k)$  of the form (32), the state of the optimal trajectory at time step  $k$ , which is obtained using (31), is

$$x_k^* = (I + C_{S,k}S_k)^{-1} (A_{S,k}x_S + b_{S,k} + C_{S,k}v_k). \quad (55)$$

The proof is provided in Appendix I-D.

## D. Extensions

In this section, the aim is to discuss some straightforward extensions of the parallel LQT.

**1) Extension to stochastic control:** Although the extension of the general framework introduced in this article to stochastic control problems is hard, the stochastic LQT case follows easily. Stochastic LQT is concerned with models of the form

$$x_{k+1} = F_kx_k + c_k + L_ku_k + G_kw_k, \quad (56)$$

$$C[u_{S:T-1}] = \mathbb{E} \left[ \ell_T(x_T) + \sum_{n=S}^{T-1} \ell_n(x_n, u_n) \right], \quad (57)$$

where  $\ell_T(x_T)$  and  $\ell_n(x_n)$  are as given in (5), and  $w_k$  is a zero mean white noise process with covariance  $Q_k$ ,  $G_k$  is a given matrix, and  $\mathbb{E}[\cdot]$  denotes expectation over the trajectories. It turns out that due to certainty equivalence property of linear stochastic control problems [1], [29], the optimal control is still given by (10) and the solution exactly matches the deterministic solution, that is, is independent of

$Q_k$  and  $G_k$ . The optimal value functions both in deterministic and stochastic cases have the form (6), but the value of the (irrelevant) constant is different.

It also results from the certainty equivalence property that the optimal control solution to the partially observed linear (affine) stochastic control problem with function (57) and dynamic and measurement models

$$x_{k+1} = F_kx_k + c_k + L_ku_k + G_kw_k, \quad (58)$$

$$y_k = O_kx_k + d_k + e_k, \quad (59)$$

where  $y_k$  is a measurement,  $O_k$  is a measurement model matrix,  $d_k$  is a deterministic bias, and  $e_k$  is a zero mean Gaussian measurement noise, is given by (10), where the state  $x_k$  is replaced with its Kalman filter estimate.

**2) Extension to more general cost functions:** Sometimes (such as in the nonlinear case below) we are interested in generalising the cost function in (5) to the following form for  $n < T$ :

$$\begin{aligned} \ell_n(x_n, u_n) &= \frac{1}{2} (H_nx_n - r_n)^\top X_n (H_nx_n - r_n) \\ &\quad + (H_nx_n - r_n)^\top M_n (u_n - s_n) \\ &\quad + \frac{1}{2} (u_n - s_n)^\top U_n (u_n - s_n) \\ &= \frac{1}{2} \begin{bmatrix} H_nx_n - r_n \\ u_n - s_n \end{bmatrix}^\top \begin{bmatrix} X_n & M_n \\ M_n^\top & U_n \end{bmatrix} \begin{bmatrix} H_nx_n - r_n \\ u_n - s_n \end{bmatrix}. \end{aligned} \quad (60)$$

We can now transform this into the form (5) by using the factorisation

$$\begin{pmatrix} X_n & M_n \\ M_n^\top & U_n \end{pmatrix} = \begin{pmatrix} I & 0 \\ U_n^{-1}M_n^\top & I \end{pmatrix}^\top \times \begin{pmatrix} X_n - M_nU_n^{-1}M_n^\top & 0 \\ 0 & U_n \end{pmatrix} \begin{pmatrix} I & 0 \\ U_n^{-1}M_n^\top & I \end{pmatrix}. \quad (61)$$

We thus have

$$\begin{aligned} &\begin{pmatrix} I & 0 \\ U_n^{-1}M_n^\top & I \end{pmatrix} \begin{pmatrix} H_nx_n - r_n \\ u_n - s_n \end{pmatrix} \\ &= \begin{pmatrix} H_nx_n - r_n \\ U_n^{-1}M_n^\top (H_nx_n - r_n) + u_n - s_n \end{pmatrix}, \end{aligned} \quad (62)$$

and by defining

$$\begin{aligned} \tilde{u}_n &= U_n^{-1}M_n^\top (H_nx_n - r_n) + u_n - s_n, \\ \tilde{F}_n &= F_n - L_nU_n^{-1}M_n^\top H_n, \\ \tilde{c}_n &= c_n + L_nU_n^{-1}M_n^\top r_n + L_ns_n, \\ \tilde{X}_n &= X_n - M_nU_n^{-1}M_n^\top, \\ \tilde{U}_n &= U_n, \end{aligned} \quad (63)$$

we get a system of the form (5), where we can solve for  $(x_n, \tilde{u}_n)$ , and the final control signal can then be recovered via

$$u_n = \tilde{u}_n - U_n^{-1}M_n^\top (H_nx_n - r_n) + s_n. \quad (64)$$

3) *Extension to nonlinear control*: The previous equations for solving the LQT problem can be extended to approximately solve nonlinear LQT systems by performing iterated linearisations, as in [21]. Let us consider a system of the form

$$\begin{aligned} x_{k+1} &= f_k(x_k, u_k), \\ \ell_n(x_n, u_n) &= \frac{1}{2}(h_n(x_n) - r_n)^\top X_n(h_n(x_n) - r_n) \\ &\quad + \frac{1}{2}(g_n(u_n) - s_n)^\top U_n(g_n(u_n) - s_n), \\ \ell_T(x_T) &= \frac{1}{2}(h_T(x_T) - r_T)^\top X_T(h_T(x_T) - r_T) \end{aligned} \quad (65)$$

where  $f_k(\cdot)$ ,  $g_n(\cdot)$  and  $h_n(\cdot)$  are possibly nonlinear functions. Given a nominal trajectory  $\bar{x}_k, \bar{u}_k$  for  $k \in S, \dots, T$ , we can linearise the nonlinear functions using first-order Taylor series as

$$\begin{aligned} f_k(x_k, u_k) &\approx f_k(\bar{x}_k, \bar{u}_k) + J_{f_k}^x(x_k - \bar{x}_k) + J_{f_k}^u(u_k - \bar{u}_k) \\ h_n(x_n) &\approx h_n(\bar{x}_n) + J_{h_n}^x(x_n - \bar{x}_n), \\ g_n(u_n) &\approx g_n(\bar{u}_n) + J_{g_n}^u(u_n - \bar{u}_n), \end{aligned} \quad (66)$$

where  $J_{f_k}^x$  represents the Jacobian of function  $f_k(\cdot)$  evaluated at  $\bar{x}_k, \bar{u}_k$  with respect to variable  $x$ .

Starting with a nominal trajectory  $\bar{x}_k^1, \bar{u}_k^1$  for  $k \in S, \dots, T$ , we linearise the system using (66), obtain the value functions using parallel scans (see Lemma 11), and obtain a new optimal trajectory  $\bar{x}_k^2$  and control  $\bar{u}_k^2$ . Then, we can repeat this procedure of linearisation and optimal trajectory/control computation until convergence. The procedure may be initialised, for example, with  $\bar{x}_k^1 = 0, \bar{u}_k^1 = 0$  or  $\bar{x}_k^1 = x_S, \bar{u}_k^1 = 0 \forall k$ .

## V. IMPLEMENTATION AND COMPUTATIONAL COMPLEXITY

In this section, we discuss the parallel implementation of the methods as well as hardware and software that were available at the time of writing for implementing the methods. We also discuss the computational complexity of the methods.

### A. Practical implementation of parallel control

Given the associative operators and the elements, the solution to the dynamic programming and trajectory prediction problems reduces to an initialisation step followed by a single call to a parallel scan algorithm routine parameterised by these operators and elements. Given the result of the scan, there might be a result-extraction step which computes the final result from the scan results. For example, LQT control law computation consists of the following steps:

- 1) *Initialisation*: Compute the elements  $A_{k,k+1}$ ,  $b_{k,k+1}$ ,  $C_{k,k+1}$ ,  $\eta_{k,k+1}$ , and  $J_{k,k+1}$  defined in Lemma 11 for all  $k$  in parallel.
- 2) *Parallel scan*: Call the backward parallel scan routine and as its arguments give the initialised elements above along with pointer to the operator given in Lemma 10.
- 3) *Extraction*: Compute the control using (10) in parallel for all  $k$ .

The control law for a finite-state control problem amounts to initialisation with the conditional value functions in Theorem 5 and the parallel scan routine is given a pointer to the operator

in Definition 3. The control law computation is finally done with (3) using the value functions computed in parallel.

Sometimes, we also need to compute the actual trajectory and the corresponding optimal controls forward in time. For example, in iterative non-linear extensions of LQT discussed in Section IV-D.3 we need to linearise the trajectory with respect to the optimal trajectory and control obtained at the previous iteration. In this case, after computing the control laws, we need to do another computational pass. For example, in the LQT case when using Method 1 from Section IV-C, we do the following:

- 1) *Initialisation*: Compute the elements  $\tilde{F}_{k,k+1}$  and  $\tilde{c}_{k,k+1}$  using Lemma 14 for all  $k$  in parallel.
- 2) *Parallel scan*: Call the forward parallel scan routine and as its arguments give the initialised elements above along with pointer to the operator given in Lemma 13.
- 3) *Extraction*: The optimal trajectory can be extracted from the forward scan results as the elements  $\tilde{c}_{S,k}$ .

The finite-state case for the Method 1 is analogous to above, but now the elements are initialised according to Lemma 9 and the combination operator is given in Definition 8.

When using Method 2 for optimal trajectory recovery, the operator is the same as in the backward computation for the control law. The parallel scan is done in forward direction and the final results still need to be evaluated at  $x_S$  unless initialisation is done using Remark 12. Furthermore, after computing the backward and forward scans, we still need to compute the optimal states by using (31) which in the case of LQT reduces to (55).

To be able to implement the aforementioned initialisations and the calls to the parallel scan routine, we need to have the parallel scan algorithm, the operators, and the elements implemented in a computer or other hardware that is capable of parallel computation. At the time of writing the most suitable hardware platforms for this purpose were multi-core CPU computers and graphics processing units (GPUs), which we discuss in next section. Other possible solutions included clusters, grids, and networked computer solutions, but their challenge was the significant communication overhead which complicates implementation of the algorithms.

### B. Implementation on multi-core CPUs and GPUs

At the time of writing, for parallel computing on CPUs the established solutions (see, e.g., [30], [31]) included thread libraries (e.g. pthreads and Java threads), message passing libraries (e.g. MPI), and share memory programming libraries (e.g. OpenMP). For GPU programming, the solutions included, for example, the CUDA library targeted for Nvidia's GPUs and the cross-platform OpenCL. However, there also were slightly higher level tools for GPU programming as, for example, the Python compiler Numba [34] was capable of generating GPU code from Python code, and Julia language [35] had a direct support for GPU computations.

Additionally, deep-learning targeted open-source libraries such as TensorFlow [36] and PyTorch [37] (developed by Google's and Facebook's research labs, respectively) provided

useful ready-developed tensor libraries which could automatically deploy computational code to GPUs. In this context tensor computing refers to generalised matrix operations which allow for computing sums, products, decompositions, and other matrix operations simultaneously to arrays (i.e., batches) of matrices or vectors, in parallel. For example, TensorFlow [36] (version 2.4 at the time of writing) was based on a parallel dataflow model implemented as a computational graph where the primitive operations were the tensor operations. The TensorFlow library itself was a set of routines to build the computational graph from the primitive operations, and the framework allowed for executing the computational graph on both CPUs and GPUs. As this library already supported parallel scans and all the required parallel matrix operations, we also implemented the methods using TensorFlow.

### C. Computational complexity

Let us now analyse the computational complexity of the proposed methods. For this purpose it is useful to assume that the computer that we have operates approximately according to the PRAM (parallel random access machine) model of computation (see, e.g., [30], [31]). In that model we assume that we have a bounded number  $P$  of identical processors controlled by a common clock with a read/write access to a shared random access memory. This model is quite accurate for multi-core CPUs and GPUs. The corresponding single-processor model is called random access machine (RAM).

For simplicity of analysis we assume that the number of processors is large enough (say  $P \rightarrow \infty$ ), so that the number of processors does not limit the parallelisation. Thus the parallel scan algorithm has a time-complexity (i.e., span-complexity) of  $O(\log T)$  in the number of associative operations. In the following we also take the dimensionality of the state into account and thus the time-complexities not only depend on the number of time steps  $T$ , but also on the number of states  $D_x$  and number of controls  $D_u$  in finite state-space case, and dimensionalities of the state  $n_x$  and control  $n_u$  in the LQT case.

In the case of finite-state system, the joint complexity of the value function iteration (2) and computation of the control law (3) on a single-processor (RAM) computer is  $O(D_x D_u T)$ . For the forward pass of the parallel finite-state system the complexity of direct sequential simulation is  $O(T)$ . For the parallel algorithms we now get the following.

*Lemma 16:* In a PRAM computer with large enough number of processors ( $P \rightarrow \infty$ ) the span time complexity of

- computing value functions and the control law for the finite-state problem is  $O(\log D_u + (\log T)(\log D_x))$ ;
- recovering the trajectory in the finite-state case with Method 1 is  $O(\log T)$  and with Method 2 it is  $O(\log D_u + \log D_x + (\log T)(\log D_x))$ .

*Proof:* The initialisation of the value function computation is done using (22) which turns out to have time (span) complexity of  $O(\log D_u)$  due to the minimisation operation over the control input. The associative operator in (3) is fully parallelisable in summation, but the span complexity of the minimisation over the state is  $O(\log D_x)$ . The control law

computation also has the complexity  $O(\log D_u)$  and hence the total span complexity follows. For trajectory recovery with Method 1 we notice that each of the steps of initialisation and associative operator application are fully parallelisable. In Method 2, the initialisation and value function computation have the same complexity as in the backward value function computation and the minimisation at the final combination step takes  $O(\log D_x)$  time. ■

In the case of LQT the time complexity of the backward value function and control law computation on RAM is  $O((n_u^3 + n_x^3)T)$  where the cubic dependencies result from LU/Cholesky factorisations and matrix-matrix products. The trajectory recovery can be sequentially done with  $O((n_x^2 + n_u^2)T)$  steps and for the parallel methods we have the following. For the parallel LQT we have the following.

*Lemma 17:* In a PRAM computer with large enough number of processors ( $P \rightarrow \infty$ ) the span time complexity of

- computing value functions and the control law for the LQT problem is  $O(n_u + n_x \log T)$ ;
- recovering the trajectory in the LQT case with Method 1 is  $O(\log n_u + (\log T)(\log n_x))$  and with Method 2 it is  $O(n_x + n_x \log T)$ .

*Proof:* A product of  $n \times n$  matrices can be computed in parallel in  $O(\log n)$  time, and an  $n \times n$  LU factorisation can be computed in parallel in  $O(n)$  time [38]. Hence the initialisation requires  $O(n_u)$  time as the contribution of the matrix products is negligible. The time complexity of the associative operator is dominated by the LU factorisations which take  $O(n_x)$  time and the matrix factorisations at the control law computation can be performed in  $O(n_u)$  time. The matrix products required in initialisation have negligible effect and therefore, the total complexity follows. In trajectory recovery Method 1, the matrix products at the initialisation can be computed in  $O(\log n_u)$  time and the associative operators in  $O(\log n_x)$  time. In Method 2, the initialisation is again negligible, and associative operations take  $O(n_x)$  time, and the final combination  $O(n_x)$  time. ■

Although the above analysis results give a guideline for performance in large number of processors (computational cores), with finite number of processors we can expect significantly worse performance as we cannot allocate a single task to single processor. However, at the time of writing the typical number of cores in a GPU was already  $\sim 10k$ , and therefore the above analysis can be expected to become more and more accurate in the future with the steadily increasing number of computational cores.

## VI. EXPERIMENTAL RESULTS

In this section we experimentally evaluate the performance of the methods in simulated applications. We implemented the methods using the open-source TensorFlow 2.4 software library [36] using its Python 3.7 interface, which provides means to run parallel vectorised operations and parallel associative scans on multi-CPU architectures and GPUs. The experiments were carried both on a CPU, AMD Ryzen™ Threadripper™ 3960X with 24 Cores of 3.8 GHz and 128 GB of RAM, and a GPU, NVIDIA® Ampere® GeForce RTX 3090 (GA102) with 10496 cores and 24 GB of RAM.



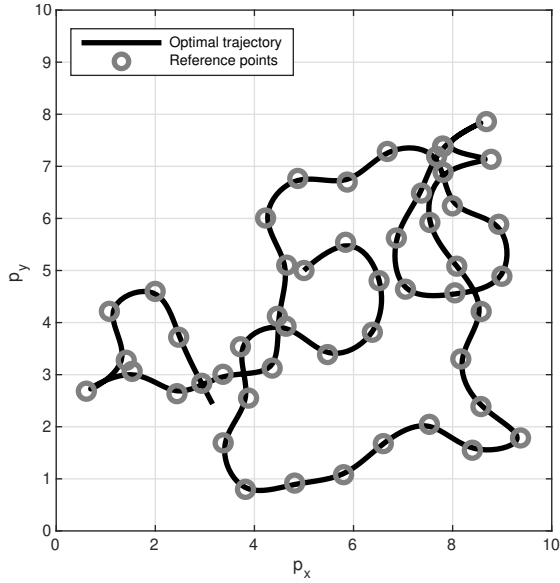


Fig. 1. Simulated trajectory from the linear control problem and optimal trajectory produced by LQT. The trajectory starts at (5, 5).

It is worth noting that both the sequential and parallel versions were implemented using TensorFlow and run on multi-core CPUs and GPUs. Because TensorFlow automatically uses parallel matrix, minimisation, and other routines, the sequential versions have also a degree of parallelisation in them. If the sequential methods had been run with a single core only, then the difference between the sequential and parallel methods would have been much larger. However, for fairness, we chose to let the sequential algorithms to take advantage of parallel computing resources as much as they can.

In the experiments we concentrate on the computational speed benefits because the sequential and parallel version of the algorithm compute exactly the same solution (provided that is unique), the only difference being in the computational speed. The computation speeds were measured by averaging over 10 runs and the time taken to (jit) compile the code was not included into the measurement.

#### A. Experiment with LQT

In this experiment we consider a 2d linear quadratic control (i.e., tracking) problem where the aim is to steer an object to follow a given trajectory of reference points in 2d by using applied forces as the control signals. The state consists of the positions and velocities  $x = [p_x \ p_y \ v_x \ v_y]^\top$  and the control signal  $u = [a_x \ a_y]^\top$  contains the accelerations (forces divided by the mass which is unity in our case). If we assume that the control signal is kept fixed over each discretisation interval  $[t_k, t_{k+1}]$ , then the dynamic model can be written as

$$x_{k+1} = F_k x_k + L_k u_k, \quad (67)$$

where

$$F_k = \begin{bmatrix} 1 & 0 & \Delta t_k & 0 \\ 0 & 1 & 0 & \Delta t_k \\ 0 & 0 & 1 & 0 \\ 0 & 0 & 0 & 1 \end{bmatrix}, L_k = \begin{bmatrix} \Delta t_k^2/2 & 0 \\ 0 & \Delta t_k^2/2 \\ \Delta t_k & 0 \\ 0 & \Delta t_k \end{bmatrix}, \quad (68)$$

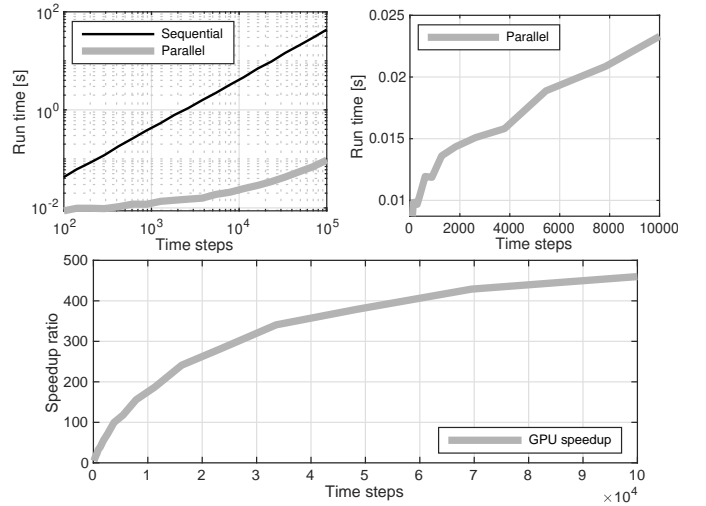


Fig. 2. LQT control law computation runtimes on GPU. The sequential and parallel run times are shown in the top left figure, and a zoom to the parallel run time is shown in the top right figure. The speedup provided by the parallelisation is shown in figure at the bottom.

and  $\Delta t_k = t_{k+1} - t_k$  is the sampling interval. Fig. 1 illustrates the scenario.

The dynamic trajectory is discretized so that we add 10 intermediate steps between each of the reference point time steps which then results in a total of  $T$  time steps (giving  $\Delta t_k = 0.1$ ). The cost function parameters are for  $k = 0, \dots, T-1$  selected to be

$$H_k = \begin{bmatrix} 1 & 0 & 0 & 0 \\ 0 & 1 & 0 & 0 \end{bmatrix}, X_k = \begin{bmatrix} c_k & 0 \\ 0 & c_k \end{bmatrix}, U_k = 10^{-1} I_{2 \times 2}, \quad (69)$$

where  $c_k = 100$  when there is a reference point at step  $k$  and  $10^{-6}$  otherwise. At the final step we set  $H_T = I_{4 \times 4}$  and  $X_T = I_{4 \times 4}$ . The reference trajectory contains the actual reference points at every 10th step  $k$ , and the intermediate steps are set equal to the previous reference point. At the final step the reference velocity is also zero. Together with the value  $c_k = 10^{-6}$  at these intermediate points this results in tiny regularisation of the intermediate paths, but the effect on the final result is practically negligible. It would also be possible to put  $c_k = 0$  for the intermediate steps to yield almost the same result.

The results computing the control law (i.e., the backward pass) of the classic sequential LQT and the proposed parallel LQT on the GPU for  $T = 10^2, \dots, 10^5$  are shown in Fig. 2. The figure shows the run times of both in log-log scale on the top left figure and the parallel result up to  $10^4$  is shown in linear scale on the top right. The speedup computed as the ratio of sequential and parallel run times is shown in the bottom figure. It can be seen that the parallel version is significantly faster than the sequential version (illustrated in the top left figure) and the logarithmic scaling of the parallel algorithm can also be seen (illustrated in the top right figure). The speedup (illustrated in the bottom figure) is of the order of  $\sim 450$  with  $10^5$  time points and although it is close to saturating, it still increases a bit.

The result of running the same experiment on the CPU is

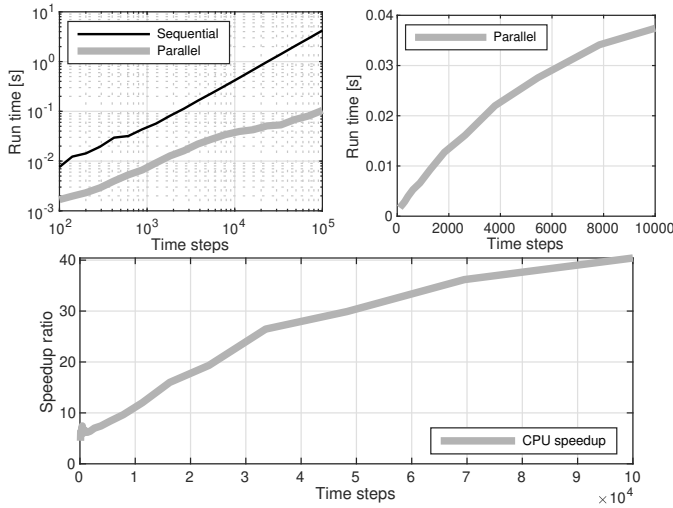


Fig. 3. LQT control law computation runtimes on CPU. The sequential and parallel run times are shown in the top left figure, and a zoom to the parallel run time is shown in the top right figure. The speedup provided by the parallelisation is shown in figure at the bottom.

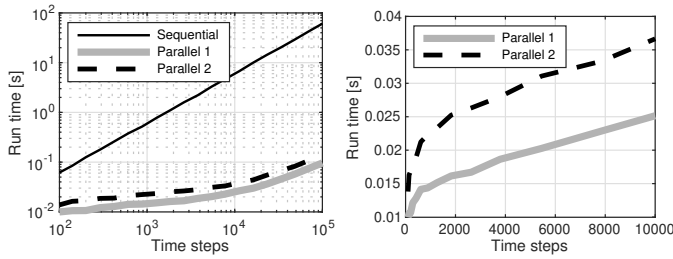


Fig. 4. The GPU run times (left) and zoomed run times of the parallel methods (right) for combined control law computation and trajectory recovery (Methods 1 & 2) in LQT.

shown in Fig. 3. Due to the multiple cores available in the CPU, the parallel version is still significantly faster than the sequential version. In this case the speedup at  $T = 10^5$  is of the order  $\sim 40$  which is actually more than the number of cores in the computer.

We also ran the combined control law computation pass and the trajectory recovery pass on both GPU and CPU and the results are shown in Figs. 4 and 5. The advantage of parallel version over the sequential version can again be clearly seen, and the difference is much more pronounced in the GPU results than in CPU results. In this case, Method 1 for the trajectory recovery is faster than Method 2 in GPU, but on

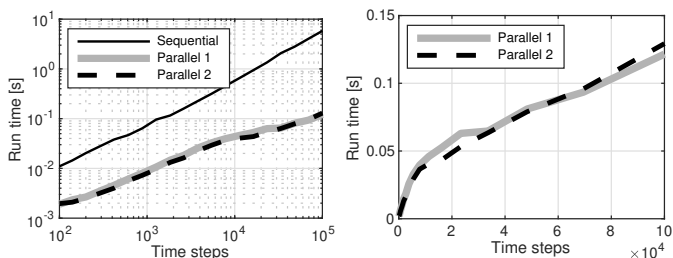


Fig. 5. The CPU run times (left) and zoomed run times of the parallel methods (right) for combined control law computation and trajectory recovery (Methods 1 & 2) in LQT.

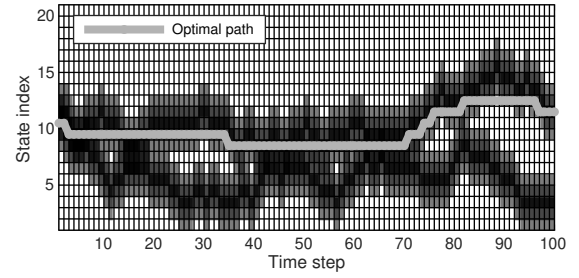


Fig. 6. Finite state space scenario where the aim is to find a minimum cost path from left to right by steering up or down. The gray scale values show the cost function values.

CPU there is no systematic difference between them.

### B. Experiment with finite state space

In this experiment we consider a finite-state game, where a flying device proceeds from left to right, and the aim is to control up and down movement on the grid so that the total cost is minimised. Each of the grid points incurs a cost  $\{0, 1, 2\}$  which is related to the roughness of the track at that point. Taking a control up or down costs single unit, and proceeding straight costs nothing. The scenario is illustrated in Fig. 6.

In this case we tested the finite-state control law computation using different state dimensionalities as the parallel combination rule can be expected to have a dependence on the state dimensionality when the number of computational cores is limited. The speedups for state dimensionalities  $D_x \in \{5, 11, 21\}$  are shown in Fig. 7 for GPU and in Fig. 8 for CPU. It can be seen that with state dimensionality  $D_x = 5$  the speedup for the GPU reaches  $\sim 4000$  with  $T = 10^5$  and is still increasing. For CPU, the speedup has grown up value  $\sim 20$  which is close to the number of available CPU cores. With the state dimensionality  $D_x = 11$  there is a drop in both speedups, and GPU speedup is already dropped to  $\sim 1100$  at  $T = 10^5$  from its peak value of  $\sim 1300$ . The CPU speedup has seemed to saturate to a value near 6. With state dimensionality  $D_x = 21$  the speedup of GPU saturates to a value around 300 and the CPU speedup saturates approximately to 1.5. However, with all of the state dimensionalities parallelisation provides a significant speedup, especially on GPU.

It should be noted that it would certainly be possible to run the experiment with higher state dimension than 21, but the GPU which we used runs out of memory with higher state dimensionalities and the given time series lengths.

### C. Experiment with nonlinear LQT

This experiment is concerned with non-linear dynamic model where we control a device whose state consists of 2d position, orientation, and speed  $x = [p_x \ p_y \ \theta \ s]^T$ . The aim is to steer the device to follow a given position and orientation trajectory which corresponds to going around a fixed race track multiple times. The control signal consists of the tangential acceleration and turn rate  $u = [a \ \omega]^T$ . The discretized nonlinear model has the form

$$x_{k+1} = f_k(x_k, u_k), \quad (70)$$

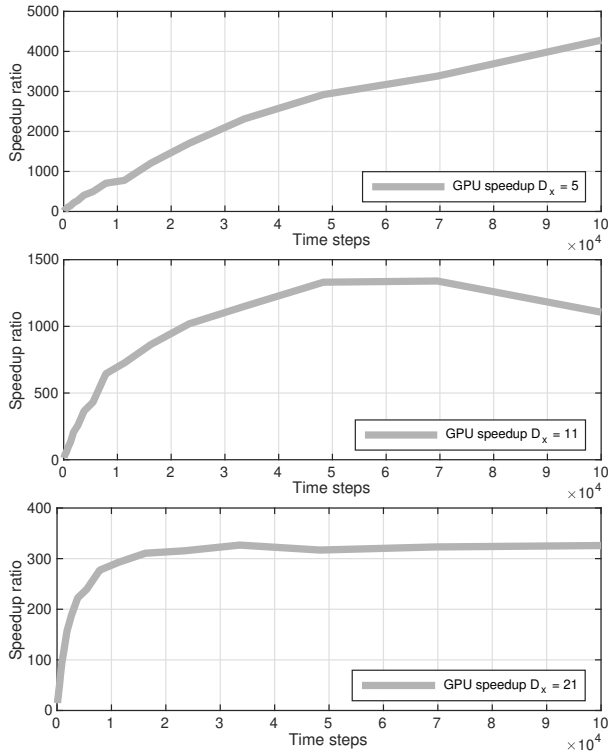


Fig. 7. Finite state space GPU speedups for control law computation (parallel vs. sequential) with state dimensions 5, 11, and 21.

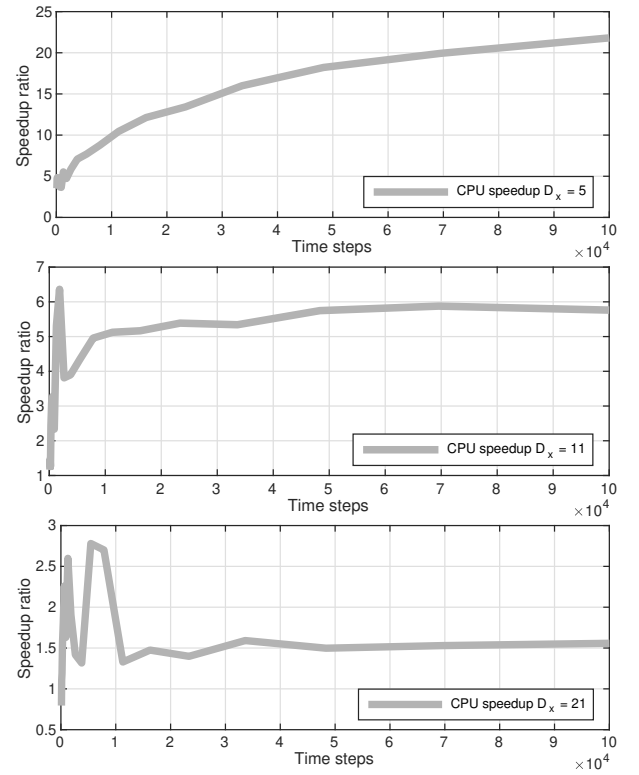


Fig. 8. Finite state space CPU speedups for control law computation (parallel vs. sequential) with state dimensions 5, 11, and 21.

where

$$f_k(x, u) = \begin{bmatrix} p_x + s \cos(\theta) \Delta t_k \\ p_y + s \sin(\theta) \Delta t_k \\ \theta + \omega \Delta t_k \\ s + a \Delta t_k \end{bmatrix}, \quad (71)$$

where  $\Delta t_k = t_{k+1} - t_k$ . Fig. 9 shows the trajectory and the optimal trajectory produced by the nonlinear LQT.

The cost function parameters were selected to be for  $k = 0, \dots, T-1$

$$H_k = \begin{bmatrix} 1 & 0 & 0 & 0 \\ 0 & 1 & 0 & 0 \\ 0 & 0 & 1 & 0 \end{bmatrix}, X_k = \begin{bmatrix} c_k & 0 & 0 \\ 0 & c_k & 0 \\ 0 & 0 & d_k \end{bmatrix}, U_k = \begin{bmatrix} 1 & 0 \\ 0 & 100 \end{bmatrix}, \quad (72)$$

where  $c_k = 100, d_k = 1000$  when there is a reference point at step  $k$  and  $10^{-6}$  otherwise. The latter values were also used for the terminal step  $k = T$ . The time step length was  $\Delta t_k = 0.1$ .

An iterated nonlinear LQT using a Taylor series approximation was applied to the model, and the number of iterations was fixed to 10. Figs. 10 and 11 show the runtimes for GPU and CPU, respectively. It can be seen that parallelisation provides a significant speedup over sequential computation. When the Method 1 was used to compute the recovered trajectory at each iteration step, the speedup grows to around 150 for  $T = 10^5$  on GPU, whereas Method 2 only reaches value around 80. On the CPU, both of the methods provide speedup between 50–60 and in this case Method 2 is slightly faster than Method 1.

## VII. CONCLUSION

In this paper, we have shown how dynamic programming solutions to optimal control problems and their linear quadratic

special case, the linear quadratic tracker (LQT), can be parallelised in the temporal domain by defining the corresponding associative operators and making use of parallel scans. The parallel methods have logarithmic complexity with respect to the number of time steps, which significantly reduces the linear complexity of standard (sequential) methods for long time horizon control problems. These benefits are shown via numerical experiments run on a CPU and GPU.

An interesting future extension of the framework would be parallel stochastic dynamic programming solution to stochastic control problems [1], [29]. As discussed in Section IV-D, this is straightforward in the LQT case due to certainty equivalence, but the general stochastic case is not straightforward. Formally it is possible to replace the state  $x_k$  with the distribution of the state  $p_k$  and consider condition value functionals of the form  $V_{i \rightarrow j}[p_i, p_j]$  and value functionals of the form  $V_i[p_i]$ . The present framework then, in principle, applies as such. In particular, when the distributions have finite-dimensional sufficient statistics, this can lead to tractable methods. Unfortunately, unlike in the sequential dynamic programming case, more generally, this approach does not seem to lead to a tractable algorithm.

Another interesting extension is to consider continuous optimal control problems in which case also the stochastic control solution has certain group properties [39] which might allow for parallelisation. However, the benefit of parallelisation in the continuous case is not as clear as in discrete-time case because of the infinite number of time steps.

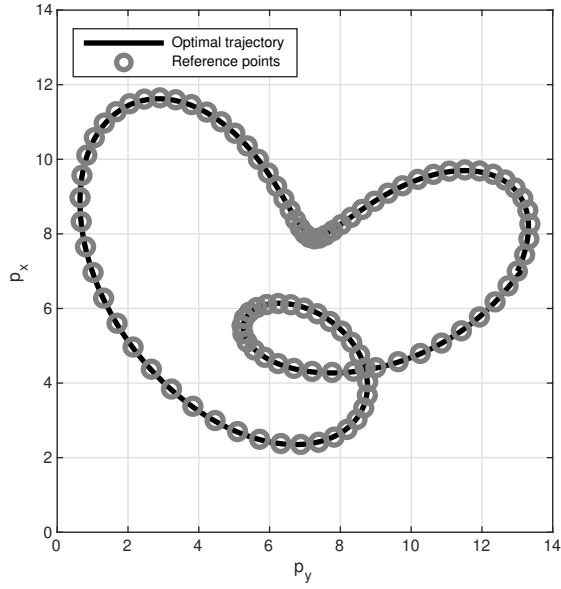


Fig. 9. Simulated trajectory from the nonlinear control problem and optimal trajectory produced by nonlinear LQT.

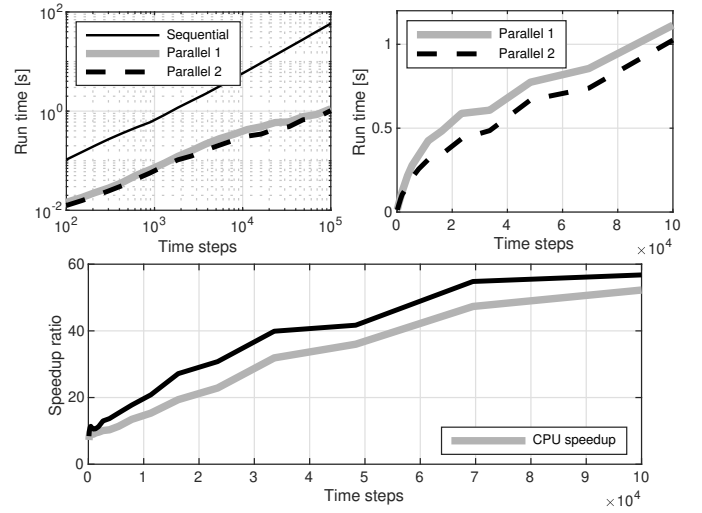


Fig. 11. Nonlinear LQT CPU runtimes and speedup for 10 iterations.

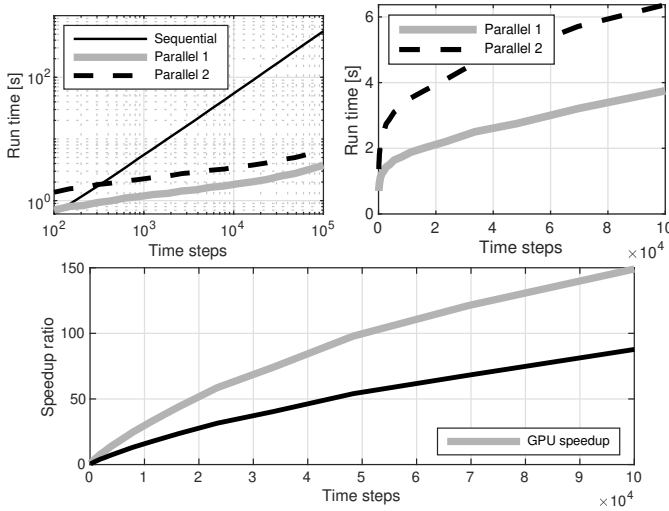


Fig. 10. Nonlinear LQT GPU runtimes and speedup for 10 iterations.

## APPENDIX I DERIVATIONS AND PROOFS

### A. Proof of Theorem 2

In this appendix we prove Theorem 2 which is concerning the combinations of conditional value functions and conventional value functions. We first prove (18). From (1) and (2),

we obtain

$$\begin{aligned}
 V_k(x_k) &= \min_{u_{k:T-1}} \ell_T(x_T) + \sum_{n=k}^{T-1} \ell_n(x_n, u_n) \\
 &= \min_{u_{k:T-1}} \sum_{n=k}^{i-1} \ell_n(x_n, u_n) + \sum_{n=i}^{T-1} \ell_n(x_n, u_n) + \ell_T(x_T) \\
 &= \min_{u_{k:i-1}} \sum_{n=k}^{i-1} \ell_n(x_n, u_n) + \min_{u_{i:T-1}} \left[ \sum_{n=i}^{T-1} \ell_n(x_n, u_n) + \ell_T(x_T) \right] \\
 &= \min_{u_{k:i-1}} \sum_{n=k}^{i-1} \ell_n(x_n, u_n) + V_i(x_i),
 \end{aligned} \tag{73}$$

where the previous minimisations are subject to the trajectory constraints in (1).

We can also minimise over  $x_i$  explicitly such that

$$V_k(x_k) = \min_{x_i} \left[ \min_{u_{k:i-1}} \left[ \sum_{n=k}^{i-1} \ell_n(x_n, u_n) \right] + V_i(x_i) \right] \tag{74}$$

$$= \min_{u_{i-1}} [V_{k \rightarrow i}(x_k, x_i) + V_i(x_i)], \tag{75}$$

which proves (18).

Proceeding analogously, we now prove (17). From (15), we



obtain

$$\begin{aligned}
& V_{k \rightarrow i}(x_k, x_i) \\
&= \min_{u_{k:i-1}} \sum_{n=k}^{i-1} \ell_n(x_n, u_n) \\
&= \min_{u_{k:j-1}} \left[ \sum_{n=k}^{j-1} L_n(x_n, u_n) + \min_{u_{j:i-1}} \sum_{n=j}^{i-1} \ell_n(x_n, u_n) \right] \\
&= \min_{u_{k:j-1}} \left[ \sum_{n=k}^{j-1} \ell_n(x_n, u_n) + V_{j \rightarrow i}(x_j, x_i) \right] \\
&= \min_{x_j} \min_{u_{k:j-1}} \left[ \sum_{n=k}^{j-1} \ell_n(x_n, u_n) + V_{j \rightarrow i}(x_j, x_i) \right] \\
&= \min_{x_j} \left[ \min_{u_{k:j-1}} \left( \sum_{n=k}^{j-1} \ell_n(x_n, u_n) \right) + V_{j \rightarrow i}(x_j, x_i) \right] \\
&= \min_{x_j} [V_{k \rightarrow j}(x_k, x_j) + V_{j \rightarrow i}(x_j, x_i)], \tag{76}
\end{aligned}$$

which completes the proof of (15).

### B. Proof of LQT combination rule

In this appendix, we prove the combination rule for LQT in Lemma 10. Combining  $V_{k \rightarrow j}(x_k, x_j)$  and  $V_{j \rightarrow i}(x_j, x_i)$  of the form (32), we obtain

$$\begin{aligned}
& V_{k \rightarrow i}(x_k, x_i) \\
&= \min_{x_j} \left\{ \max_{\lambda_1} g_{k \rightarrow j}(\lambda_1; x_k, x_j) + \max_{\lambda_2} g_{j \rightarrow i}(\lambda_2; x_j, x_i) \right\} \\
&= z + \max_{\lambda_1, \lambda_2} \min_{x_j} \left\{ \frac{1}{2} x_k^\top J_{k,j} x_k - x_k^\top \eta_{k,j} - \frac{1}{2} \lambda_1^\top C_{k,j} \lambda_1 \right. \\
&\quad - \lambda_1^\top (x_j - A_{k,j} x_k - b_{k,j}) + \frac{1}{2} x_j^\top J_{j,i} x_j - x_j^\top \eta_{j,i} \\
&\quad \left. - \frac{1}{2} \lambda_2^\top C_{j,i} \lambda_2 - \lambda_2^\top (x_i - A_{j,i} x_j - b_{j,i}) \right\}.
\end{aligned}$$

We prove the result by calculating the minimum w.r.t.  $x_j$  and maximum w.r.t.  $\lambda_1$ , leaving the Lagrange multiplier  $\lambda_2$  as the Lagrange multiplier of  $V_{k \rightarrow i}(x_k, x_i)$ .

Setting the gradient w.r.t.  $x_j$  equal to zero, we obtain

$$J_{j,i} x_j = \lambda_1 + \eta_{j,i} - A_{j,i}^\top \lambda_2, \tag{77}$$

where  $J_{j,i}$  is not invertible in general.

Setting the gradient w.r.t.  $\lambda_1$  equal to zero, we have

$$x_j = -C_{k,j} \lambda_1 + A_{k,j} x_k + b_{k,j}. \tag{78}$$

Then, substituting (78) into (77) yields

$$\lambda_1 = (I + J_{j,i} C_{k,j})^{-1} [-\eta_{j,i} + A_{j,i}^\top \lambda_2 + J_{j,i} (A_{k,j} x_k + b_{k,j})]. \tag{79}$$

Substituting (79) into (78), we obtain

$$\begin{aligned}
x_j &= -C_{k,j} (I + J_{j,i} C_{k,j})^{-1} A_{j,i}^\top \lambda_2 \\
&\quad - C_{k,j} (I + J_{j,i} C_{k,j})^{-1} [-\eta_{j,i} + J_{j,i} (A_{k,j} x_k + b_{k,j})] \\
&\quad + A_{k,j} x_k + b_{k,j}. \tag{80}
\end{aligned}$$

We now substitute the stationary points (79) and (80) in each of the terms in  $V_{k \rightarrow i}(x_k, x_i)$  to recover a function of the

form (32). This step involves the use of long mathematical expressions so it is left out of the paper. Lemma 10 then follows by term identification.

### C. Proof of Parallel LQT

In this section, we prove Lemma 11.

**1) Proof of (40):** We first show the form of  $V_{k \rightarrow k+1}(x_k, x_{k+1})$  in its dual representation for  $k = S, \dots, T$ . Using (15) and the LQT problem formulation in (5), we obtain

$$\begin{aligned}
& V_{k \rightarrow k+1}(x_k, x_{k+1}) \\
&= \min_{u_k} \ell_k(x_k, u_k) \\
&= \min_{u_k} \frac{1}{2} (H_k x_k - r_k)^\top X_k (H_k x_k - r_k) + \frac{1}{2} u_k^\top U_k u_k \\
&= z + \min_{u_k} \frac{1}{2} x_k^\top H_k^\top X_k H_k x_k - x_k^\top H_k^\top X_k r_k + \frac{1}{2} u_k^\top U_k u_k \tag{81}
\end{aligned}$$

subject to

$$x_{k+1} = F_k x_k + c_k + L_k u_k. \tag{82}$$

The Lagrangian of  $V_{k \rightarrow k+1}(x_k, x_{k+1})$  is [20]

$$\begin{aligned}
& L_{k \rightarrow k+1}(u_k, \lambda; x_k, x_{k+1}) \\
&= z + \frac{1}{2} x_k^\top H_k^\top X_k H_k x_k - x_k^\top H_k^\top X_k r_k \\
&\quad + \frac{1}{2} u_k^\top U_k u_k + \lambda^\top (L_k u_k - (x_{k+1} - F_k x_k - c_k))
\end{aligned}$$

and the dual function is [20]

$$\begin{aligned}
& g_{k \rightarrow k+1}(\lambda; x_k, x_{k+1}) \\
&= \min_{u_k} L_{k \rightarrow k+1}(u_k, \lambda; x_k, x_{k+1}) \\
&= z + \frac{1}{2} x_k^\top H_k^\top X_k H_k x_k - x_k^\top H_k^\top X_k r_k \\
&\quad - \frac{1}{2} \lambda^\top L_k U_k^{-1} L_k^\top \lambda - \lambda^\top (x_{k+1} - F_k x_k - c_k), \tag{83}
\end{aligned}$$

where the minimum is obtained setting the gradient of  $L_{k \rightarrow k+1}(\cdot)$  w.r.t.  $u_k$  equal to zero, which gives

$$u_k = -U_k^{-1} L_k \lambda. \tag{84}$$

Comparing (83) with (33) proves the initialisation in (38). Then, by applying Theorem 2, which is equivalent to Lemma 10 in the LQT setting, we complete the proof of (40).

**2) Proof of (41):** We use induction backwards to prove (41). At the last time step, from Lemma 11, we have

$$\begin{aligned}
& V_{T \rightarrow T+1}(x_T, x_{T+1}) \\
&= \max_{\lambda} \left[ z + \frac{1}{2} x_T^\top H_T^\top X_T H_T x_T - x_T^\top H_T^\top r_T - \lambda^\top x_{T+1} \right].
\end{aligned}$$

For  $x_{T+1} \neq 0$ , this function is infinite. For  $x_{T+1} = 0$ , we have

$$V_{T \rightarrow T+1}(x_T, 0) = \frac{1}{2} x_T^\top H_T^\top X_T H_T x_T - x_T^\top H_T^\top r_T$$

which coincides with  $V_T(x_T)$ , see Section II-B.

We now assume that (41) holds for  $k + 1$ , which implies that we have

$$\begin{aligned} A_{k+1,T+1} &= 0, \\ b_{k+1,T+1} &= 0, \\ C_{k+1,T+1} &= 0, \\ \eta_{k+1,T+1} &= v_{k+1}, \\ J_{k+1,T+1} &= S_{k+1}, \end{aligned}$$

where  $v_{k+1}$  and  $S_{k+1}$  are the parameters in (6), and then show that (41) holds for  $k$ . From Lemma 11, we have

$$\begin{aligned} A_{k,k+1} &= F_k, \\ b_{k,k+1} &= c_k, \\ C_{k,k+1} &= L_k U_k^{-1} L_k^\top, \\ \eta_{k,k+1} &= H_k^\top X_k r_k, \\ J_{k,k+1} &= H_k^\top X_k H_k. \end{aligned}$$

By applying the combination rules in Lemma 10, we obtain

$$\begin{aligned} A_{k,T+1} &= 0, \\ b_{k,T+1} &= 0, \\ C_{k,T+1} &= 0, \\ \eta_{k,T+1} &= F_k^\top (I + S_{k+1} L_k U_k^{-1} L_k^\top)^{-1} (v_{k+1} - S_{k+1} c_k) \\ &\quad + H_k^\top X_k r_k, \\ J_{k,T+1} &= F_k^\top (I + S_{k+1} L_k U_k^{-1} L_k^\top)^{-1} S_{k+1} F_k + H_k^\top X_k H_k. \end{aligned} \quad (85)$$

We need to prove that these equations are equivalent to (7) and (8). We first prove that  $\eta_{k,T+1} = v_k$ , which requires proving that the following identity holds

$$F_k^\top (I + S_{k+1} L_k U_k^{-1} L_k^\top)^{-1} = (F_k^\top - L_k K_k)^\top. \quad (86)$$

On one hand, the right hand side can be written as

$$(F_k^\top - L_k K_k)^\top = F_k^\top - F_k^\top S_{k+1} L_k (L_k^\top S_{k+1} L_k + U_k)^{-1} L_k^\top. \quad (87)$$

On the other hand, by applying the matrix inversion lemma, the left-hand side becomes

$$\begin{aligned} &F_k^\top (I + S_{k+1} L_k U_k^{-1} L_k^\top)^{-1} \\ &= F_k^\top \left( I - S_{k+1} L_k (U_k + L_k^\top S_{k+1} L_k)^{-1} L_k^\top \right), \end{aligned} \quad (88)$$

which proves  $\eta_{k,T+1} = v_k$ .

To prove that  $J_{k,T+1} = S_k$ , we need to prove that

$$F_k^\top (I + S_{k+1} L_k U_k^{-1} L_k^\top)^{-1} S_{k+1} F_k = F_k^\top S_{k+1} (F_k - L_k K_k). \quad (89)$$

On one hand, the right-hand side can be written as

$$\begin{aligned} &F_k^\top S_{k+1} (F_k - L_k K_k) \\ &= F_k^\top S_{k+1} \left( F_k - L_k (L_k^\top S_{k+1} L_k + U_k)^{-1} L_k^\top S_{k+1} F_k \right) \\ &= F_k^\top S_{k+1} F_k - F_k^\top S_{k+1} L_k (L_k^\top S_{k+1} L_k + U_k)^{-1} L_k^\top S_{k+1} F_k. \end{aligned} \quad (90)$$

On the other hand, using (88), the left-hand side is

$$\begin{aligned} &F_k^\top (I + S_{k+1} L_k U_k^{-1} L_k^\top)^{-1} S_{k+1} F_k \\ &= F_k^\top \left( I - S_{k+1} L_k (U_k + L_k^\top S_{k+1} L_k)^{-1} L_k^\top \right) S_{k+1} F_k \\ &= F_k^\top S_{k+1} F_k - F_k^\top S_{k+1} L_k (U_k + L_k^\top S_{k+1} L_k)^{-1} L_k^\top S_{k+1} F_k, \end{aligned} \quad (91)$$

which proves the result.

#### D. Proof of optimal trajectory recovery

In this appendix, we prove Lemma 15. Substituting  $V_k(x_k)$  of the form (6) and  $V_{S \rightarrow k}(x_S, x_k)$  of the form (32) into (31), we obtain

$$\begin{aligned} x_k^* &= \arg \min_{x_k} \max_{\lambda} \frac{1}{2} x_S^\top J_{S,k} x_S - x_S^\top \eta_{S,k} \\ &\quad - \frac{1}{2} \lambda^\top C_{S,k} \lambda - \lambda^\top (x_k - A_{S,k} x_S - b_{S,k}) \\ &\quad + \frac{1}{2} x_k^\top S_k x_k - v_k^\top x_k. \end{aligned} \quad (92)$$

The minimum of (92) w.r.t.  $x_k$  can be found by setting the gradient of the function equal to zero, which yields

$$x_k = S_k^{-1} (\lambda + v_k). \quad (93)$$

We substitute (93) into the function (without argmin) in (92) to obtain

$$\begin{aligned} &\max_{\lambda} \frac{1}{2} x_S^\top J_{S,k} x_S - x_S^\top \eta_{S,k} - \frac{1}{2} \lambda^\top (C_{S,k} + S_k^{-1}) \lambda \\ &\quad + v_k^\top S_k^{-1} v_k - \lambda^\top (S_k^{-1} v_k - A_{S,k} x_S - b_{S,k}). \end{aligned}$$

Making the gradient of this function w.r.t.  $\lambda$  equal to zero, we obtain that the maximum is obtained for

$$\lambda = (C_{S,k} + S_k^{-1})^{-1} (-S_k^{-1} v_k + A_{S,k} x_S + b_{S,k}). \quad (94)$$

Substituting (94) into (93), we obtain (55), which finishes the proof of Lemma 15.

#### REFERENCES

- [1] R. F. Stengel, *Optimal Control and Estimation*. Dover publications, 1994.
- [2] F. L. Lewis and V. L. Syrmos, *Optimal Control*, 2nd ed. John Wiley & Sons, 1995.
- [3] D. P. Bertsekas, *Dynamic Programming and Optimal Control*, 3rd ed. Athena Scientific, 2005.
- [4] J. Biggs and W. Holderbaum, "Optimal kinematic control of an autonomous underwater vehicle," *IEEE Transactions on Automatic Control*, vol. 54, no. 7, pp. 1623–1626, 2009.
- [5] A. Komae and A. Bensoussan, "Optimal control of hidden Markov models with binary observations," *IEEE Transactions on Automatic Control*, vol. 59, no. 1, pp. 64–77, 2014.
- [6] G. Zhao and M. Zhu, "Pareto optimal multi-robot motion planning," *IEEE Transactions on Automatic Control*, 2021, in press.
- [7] R. S. Sutton and A. G. Barto, *Reinforcement Learning: An Introduction*, 2nd ed. MIT Press, 2018.
- [8] R. Bellman, *Dynamic Programming*. Princeton University Press, 1957.
- [9] R. E. Bellman and S. E. Dreyfus, "Applied dynamic programming," The RAND Corporation, Tech. Rep. R-352-PR, 1962.
- [10] A. Pakniyat and P. E. Caines, "On the relation between the minimum principle and dynamic programming for classical and hybrid control systems," *IEEE Transactions on Automatic Control*, vol. 62, no. 9, pp. 4347–4362, 2017.
- [11] S. Dormido Canto, A. P. de Madrid, and S. Dormido Bencomo, "Parallel dynamic programming on clusters of workstations," *IEEE Transactions on Parallel and Distributed Systems*, vol. 16, no. 9, pp. 785–798, 2005.

- [12] M. Gengler, "An introduction to parallel dynamic programming," in *Solving Combinatorial Optimization Problems in Parallel*. Springer, 1996, pp. 87–114.
- [13] J. Casti, M. Richardson, and R. Larson, "Dynamic programming and parallel computers," *Journal of Optimization Theory and Applications*, vol. 12, no. 4, pp. 423–438, 1973.
- [14] S. J. Wright, "Partitioned dynamic programming for optimal control," *SIAM Journal on Optimization*, vol. 1, no. 4, pp. 620–642, 1991.
- [15] S. Shin, T. Faulwasser, M. Zanon, and V. M. Zavala, "A parallel decomposition scheme for solving long-horizon optimal control problems," in *2019 IEEE 58th Conference on Decision and Control (CDC)*. IEEE, 2019, pp. 5264–5271.
- [16] Y. Jiang, J. Oravec, B. Houska, and M. Kvasnica, "Parallel MPC for linear systems with input constraints," *IEEE Transactions on Automatic Control*, 2021, in press.
- [17] J. L. Calvet and G. Viargues, "Invariant imbedding and parallelism in dynamic programming for feedback control," *Journal of Optimization Theory and Applications*, vol. 87, no. 1, pp. 121–140, 1995.
- [18] G. E. Blelloch, "Scans as primitive parallel operations," *IEEE Transactions on Computers*, vol. 38, no. 11, pp. 1526–1538, 1989.
- [19] —, "Prefix sums and their applications," School of Computer Science, Carnegie Mellon University, Tech. Rep. CMU-CS-90-190, 1990.
- [20] S. Boyd and L. Vandenberghe, *Convex Optimization*. Cambridge University Press, 2004.
- [21] W. Li and E. Todorov, "Iterative linear quadratic regulator design for nonlinear biological movement systems," in *ICINCO (1)*, 2004, pp. 222–229.
- [22] S. Särkkä and A. F. García-Fernández, "Temporal parallelization of Bayesian smoothers," *IEEE Transactions on Automatic Control*, vol. 66, pp. 299–306, 2021.
- [23] F. Yaghoobi, A. Corenflos, S. Hassan, and S. Särkkä, "Parallel iterated extended and sigma-point Kalman smoothers," in *To appear in Proceedings of IEEE International Conference on Acoustics, Speech and Signal Processing (ICASSP)*, 2021.
- [24] S. Hassan, S. Särkkä, and A. F. García-Fernández, "Temporal parallelization of inference in hidden Markov models," arXiv:2102.05743, 2021.
- [25] P. M. Dower, W. M. McEneaney, and H. Zhang, "Max-plus fundamental solution semigroups for optimal control problems," in *2015 Proceedings of the Conference on Control and its Applications*. SIAM, 2015, pp. 368–375.
- [26] H. Zhang and P. M. Dower, "Max-plus fundamental solution semigroups for a class of difference Riccati equations," *Automatica*, vol. 52, pp. 103–110, 2015.
- [27] —, "A max-plus based fundamental solution for a class of discrete time linear regulator problems," *Linear Algebra and its Applications*, vol. 471, pp. 693–729, 2015.
- [28] J. Xu, T. van den Boom, and B. De Schutter, "Model predictive control for stochastic max-plus linear systems with chance constraints," *IEEE Transactions on Automatic Control*, vol. 64, no. 1, pp. 337–342, 2019.
- [29] P. S. Maybeck, *Stochastic Models, Estimation and Control*. New York, NY: Academic Press, 1982, vol. 3.
- [30] T. Rauber and G. Rünger, *Parallel programming: For multicore and cluster systems*, 2nd ed. Springer, 2013.
- [31] G. Barlas, *Multicore and GPU Programming: An Integrated Approach*. Morgan Kaufmann Publishers Inc., 2015.
- [32] T. M. Apostol, *Calculus. Volume I*. John Wiley & Sons, 1967.
- [33] D. Koller and N. Friedman, *Probabilistic Graphical Models: Principles and Techniques*. The MIT Press, 2009.
- [34] S. K. Lam, A. Pitrou, and S. Seibert, "Numba: A llvm-based python jit compiler," in *Proceedings of the Second Workshop on the LLVM Compiler Infrastructure in HPC*, 2015, pp. 1–6.
- [35] J. Bezanson, A. Edelman, S. Karpinski, and V. B. Shah, "Julia: A fresh approach to numerical computing," *SIAM Review*, vol. 59, no. 1, pp. 65–98, 2017.
- [36] M. Abadi *et al.*, "TensorFlow: Large-scale machine learning on heterogeneous systems," 2015, software available from tensorflow.org. [Online]. Available: <https://www.tensorflow.org/>
- [37] A. Paszke, S. Gross, F. Massa, A. Lerer, J. Bradbury, G. Chanan, T. Killeen, Z. Lin, N. Gimelshein, L. Antiga, A. Desmaison, A. Kopf, E. Yang, Z. DeVito, M. Raison, A. Tejani, S. Chilamkurthy, B. Steiner, L. Fang, J. Bai, and S. Chintala, "PyTorch: An imperative style, high-performance deep learning library," in *Advances in Neural Information Processing Systems 32*, 2019, pp. 8024–8035.
- [38] J. M. Ortega, *Introduction to parallel and vector solution of linear systems*. Springer Science & Business Media, 1988.
- [39] M. Nisio, *Stochastic control theory: Dynamic programming principle*. Springer, 2015.



**Simo Särkkä** received his Master of Science (Tech.) degree (with distinction) in engineering physics and mathematics, and Doctor of Science (Tech.) degree (with distinction) in electrical and communications engineering from Helsinki University of Technology, Espoo, Finland, in 2000 and 2006, respectively. Currently, Dr. Särkkä is an Associate Professor with Aalto University and an Adjunct Professor with Tampere University of Technology and Lappeenranta University of Technology. His research interests are in multi-sensor data processing systems with applications in location sensing, health and medical technology, machine learning, inverse problems, and brain imaging. He has authored or coauthored over 150 peer-reviewed scientific articles and his books "Bayesian Filtering and Smoothing" and "Applied Stochastic Differential Equations" along with the Chinese translation of the former were recently published via the Cambridge University Press. He is a Senior Member of IEEE and serving as an Senior Area Editor of IEEE Signal Processing Letters.



**Ángel F. García-Fernández** received the telecommunication engineering degree (with honours) and the Ph.D. degree from Universidad Politécnica de Madrid, Madrid, Spain, in 2007 and 2011, respectively. He is currently a Lecturer in the Department of Electrical Engineering and Electronics at the University of Liverpool, Liverpool, UK. He previously held postdoctoral positions at Universidad Politécnica de Madrid, Chalmers University of Technology, Gothenburg, Sweden, Curtin University, Perth, Australia, and Aalto University, Espoo, Finland. His main research activities and interests are in the area of Bayesian estimation, with emphasis on dynamic systems and multiple target tracking. He was the recipient of the best paper award at the International Conference on Information Fusion in 2017 and 2019.